Positive selection within the genomes of SARS-CoV-2 and other Coronaviruses independent of impact on protein function

Alejandro Berrio[1], Valerie Gartner[1], Gregory A Wray[1,2]

[1] Biology, Duke University, Durham, North Carolina, United States

[2] Center for Genomic and Computational Biology, Duke University, Durham, North Carolina, United States

Corresponding Author:

Alejandro Berrio[1]

130 Science Drive, Durham, North Carolina, 27708, United States

Email address: alejo.berrio@duke.edu

Abstract

Background. The emergence of a novel coronavirus (SARS-CoV-2) associated with severe acute respiratory disease (COVID-19) has prompted efforts to understand the genetic basis for its unique characteristics and its jump from non-primate hosts to humans. Tests for positive selection can identify apparently nonrandom patterns of mutation accumulation within genomes, highlighting regions where molecular function may have changed during the origin of a species. Several recent studies of the SARS-CoV-2 genome have identified signals of conservation and positive selection within the gene encoding Spike protein based on the ratio of synonymous to nonsynonymous substitution. Such tests cannot, however, detect changes in the function of RNA molecules.

Methods. Here we apply a test for branch-specific oversubstitution of mutations within narrow windows of the genome without reference to the genetic code.

Results. We recapitulate the finding that the gene encoding Spike protein has been a target of both purifying and positive selection. In addition, we find other likely targets of positive selection within the genome of SARS-CoV-2, specifically within the genes encoding Nsp4 and Nsp16. Homology-directed modeling indicates no change in either Nsp4 or Nsp16 protein structure relative to the most recent common ancestor. Thermodynamic modeling of RNA stability and structure, however, indicates that RNA secondary structure within both genes in the SARS-CoV-2 genome differs from those of RaTG13, the reconstructed common ancestor, and Pan-CoV-GD (Guangdong). These SARS-CoV-2-specific mutations may affect molecular processes mediated by the positive or negative RNA molecules, including transcription, translation, RNA stability, and evasion of the host innate immune system. Our results highlight the importance of considering mutations in viral genomes not only from the perspective of their impact on protein structure, but also how they may impact other molecular processes critical to the viral life cycle.

Introduction

An important challenge in understanding zoonotic events is identifying the genetic changes that allow a pathogen to infect a new host. Such information can highlight molecular processes in both the pathogen and host that have practical value. The recent outbreak of SARS-CoV-2, a novel coronavirus, provides both a challenge and an opportunity to learn more about the specific adaptations that enable the virus to thrive in human hosts and that endow it with traits distinct from previously described coronaviruses. Formal tests for natural selection are a powerful tool in this endeavor because they can be applied in an unbiased manner throughout the viral genome: evidence of negative selection can reveal regions of the genome that are broadly constrained functionally and thus unlikely to contribute to species-specific traits, while evidence of branch-specific positive selection can identify candidate regions of the genome where molecular processes may have diverged from that of other species.

Several recent studies have tested for natural selection in the SARS-CoV-2 genome based on the ratio of synonymous to non-synonymous (dN/dS) substitutions relative to other coronaviruses (Tang et al., 2020; Chaw et al., 2020; Li et al., 2020a). The most prominent signal to emerge from these studies is a mix of positive and purifying selection within the gene encoding the Spike glycoprotein, which mediates invasion of host cells by binding to the angiotensin-converting

enzyme 2 (ACE2) receptor in host cells (Gallagher & Buchmeier, 2001; Tortorici & Veesler, 2019). This finding makes good biological sense, because structural changes in the spike protein are common and are known to influence the ability of the virus to infect new hosts and jump between species (Hulswit, de Haan & Bosch, 2016). A single nucleotide polymorphism (SNP) that results in an amino acid substitution in Spike protein has increased in frequency during the global pandemic more rapidly than other SNPs (Korber et al., 2020), leading to speculation that it is an adaptation that alters the interaction between Spike and ACE2, FURIN and TMPRSS2 (Eaaswarkhanth, Al Madhoun & Al-Mulla, 2020).

Beyond mutations that alter Spike protein, however, there exists little understanding of positive selection within the SARS-CoV-2 genome and how this may have shaped viral traits. Few convincing signals of positive selection exist for any of the other viral proteins (Cagliani et al., 2020; Velazquez-Salinas et al., 2020; Chaw et al., 2020). For RNA viruses, however, critical aspects of the life cycle rely on molecular processes that are not reflected in protein sequence. In particular, in positive-strand RNA viruses such as coronaviruses, the single RNA molecule that constitutes the genome is first transcribed and translated to produce the replicase polyprotein 1a and 1ab that is cleaved into multiple non-structural proteins, some of which participate in the assembly of a cellular structure known as the replicase-transcriptase complex (RTC), where the proper environment for viral replication and transcription is created. Then, the RNA-dependent-RNA-polymerase (RdRp or Nsp12) produces negative sense genomic and subgenomic RNAs that are used as template strands that are then transcribed in the opposite direction to make more positive-sense viral genomes and a variety of RNA molecules that are translated into structural proteins for packaging (Fehr & Perlman, 2015; Kim et al., 2020). Although the viral proteins that help mediate these processes are visible to tests for selection that rely on dN/dS ratios, the RNA molecules with which they interact are not. This leaves the operation of natural selection on important molecular functions within the viral life cycle largely unexamined.

Here we utilize a test for positive selection that identifies an excess of nucleotide substitutions within a defined window in the genome relative to neutral expectation using a likelihood ratio framework (Wong & Nielsen, 2004; Haygood et al., 2007). We implemented this test using *adaptiPhy* (Berrio, Haygood & Wray, 2020) to infer regions of the genome that were likely targets of branch-specific positive selection in several *Sarbecovirus* species from bat, pangolin, and human hosts. Our results recapitulate results from dN/dS-based tests that highlight *S*, the

gene encoding Spike protein, as a prominent target of natural selection within the SARS-CoV-2 genome (Cagliani et al., 2020; Chaw et al., 2020; Li et al., 2020a). Importantly, we also identify genomic regions not previously reported to be targets of positive selection. Based on structural modeling of RNA and protein, we argue that these newly identified regions of positive selection likely affect species-specific RNA, rather than protein, function. These genomic regions are candidates for understanding the molecular mechanisms that endow SARS-CoV-2 with some of its unique biological properties.

Materials & Methods

Sequence Alignment

To identify branch specific positive selection, it is necessary to obtain a query and a reference alignment. We downloaded six high quality reference genomes from the subgenus Sarbecovirus (Table 1). Next, we used MAFFT (Katoh & Standley, 2013) plugin in Geneious Prime v.2.1 (Kearse et al., 2012) with default settings to build a sequence alignment. Next, we refined the alignment using a gene by gene procedure.

Testing for Positive Selection

Despite *adaptiPhy* was originally designed to investigate regions of complex genomes under positive selection, it can be used to identify regions of a viral sequence alignment where the foreground branch is evolving at faster rates than the expectation from the background species. We performed a selection analysis on sliding windows of 300 bp with a step of 150 bp along a sequence alignment of 5 reference genome sequences of coronaviruses of the subgenus *Sarbecovirus* and two sequences of Pangolin Coronavirus recently published (Liu, Chen & Chen, 2019; Lam et al., 2020). This procedure generates partitions where a tree topology can be fitted. To investigate the extent of positive selection or branches with long substitution rates along the SARS-CoV-2 genome, we used a branch-specific method known as *adaptiPhy* that was initially developed in 2007 (Haygood et al., 2007) and recently improved (Berrio, Haygood & Wray, 2020). This computational methodology makes use of a likelihood ratio test based on the maximum likelihood estimates obtained from HyPhy v2.5 (Pond, Frost & Muse, 2005; Pond et al., 2020). The branch of interest (e.g., SARS-CoV-2 branch) is used as the foreground and the rest of the alignment is used as the background. To obtain data from nucleotide substitutions alone, we used *msa_split* from PHAST (Hubisz, Pollard & Siepel, 2011) to remove insertions

and any sequence gaps that were present in the genomes of the background virus species relative to the SARS-CoV-2 genome.The assumption for the background species is the same for both the null and alternative models; specifically, only neutral evolution and negative (purifying) selection are permitted. While in the foreground, the assumptions are the same as for the background in the null model. In the alternative model, all three types of evolution are permitted (neutral evolution, negative selection, and positive selection) in the foreground of the following topology: (((((SARS_CoV_2, Bat_CoV_RaTG13), Pa_CoV_Guangdong), Pa_CoV_Guangxi_P4L), (Bat_CoV_LYRa11, SARS_CoV)), Bat_CoV_BM48). This method is highly sensitive and specific and can differentiate between positive selection and relaxation of constraint. *AdaptiPhy* requires at least 3 kb reference alignment for each species that is used as a putatively neutral proxy for computing substitution rates. Viruses' genomes lack non-functional regions, therefore, the most reasonable proxy for neutral evolution has to be found in the regions outside the query window. To do this, we concatenated twenty regions of 300 bp of the viral genome alignment that were drawn randomly with replacement from the entire genome alignment. Then, for each query alignment, we built a reference alignment of 6 kb as it produces a stable evolutionary standard of recombination rates. To control for the stochasticity of the evolutionary process, we run each query against ten bootstrapped samples of reference alignments. Finally, we used a custom R script to compute the likelihood ratio, which was used as a test statistic for a chi-squared test with one degree of freedom to calculate a *P*-value for each query. Then, we corrected the distribution of all *P*-values per query region using the *p.adjust()* R function with the fdr method. Next, we classified a query window to be under positive selection if the *P*-adjusted value was < 0.05. We were unable to successfully run adaptiPhy on two windows because the outgroup species (Bat_CoV_BM48) contained a deletion of 406 bp relative to SARS-CoV-2, which spans the entire ORF8.

Next, we calculated the distribution of substitution rates for each branch and nodes in each query and reference sequence using *phyloFit* (Hubisz, Pollard & Siepel, 2011). To visualize the strength of selection comprehensively, we computed the statistic ζ (zeta), representing the evolutionary rate. To calculate this rate, we compared the substitution rate in the query with their respective reference alignments. This parameter, "ζ", is analogous to ω (omega), the ratio of dN/dS, where a value of $\omega<1$ indicates constraint or negative selection; a value of $\omega=1$ indicates neutrality; and a value of $\omega>1$ indicates positive selection (Wong & Nielsen, 2004).

Testing for Conservation

To test for conservation, we used the *phastCons* computational method from PHAST (Siepel et al., 2005; Hubisz, Pollard & Siepel, 2011). To run this tool, we used the models obtained with *phyloFit* for the reference alignments and then, we generated an average estimate of the conserved and non-conserved states of the models with *phyloBoot* (Hubisz, Pollard & Siepel, 2011). Finally, we run the final analysis using *phastCons* on the query alignments using the previous models to generate *phastCons* values for each base-pair along the sequence. To plot these we took the average from each alignment and plot it using the library Gviz and Bioconductor (Hahne & Ivanek, 2016) in R.

Testing for Recombination

Inference of branch specific selection can be confounded by recombination given that a single phylogenetic tree may not explain the evolution of viruses. Recombination is common in coronaviruses (Hon et al., 2008; Graham & Baric, 2010; Lau et al., 2015; Hu et al., 2017; Li et al., 2020b; Lam et al., 2020) and it should be accounted for as an alternative explanation of selection at the nucleotide level. Here, we screened for evidence of recombination in two ways, one, by estimating phylogenetic trees in sliding windows of 500 bp and a step of 150 along coronavirus alignment using RaXML-NG v0.9 (Kozlov et al., 2019).

Evaluating polymorphic diversity in the pandemics of 2020

We downloaded complete sequences of SARS-CoV-2 genomes from the NCBI Virus database (https://www.ncbi.nlm.nih.gov/labs/virus/vssi/#/virus?SeqType_s=Nucleotide). As of June 26, 2020, we obtained and aligned 5597 SARS-CoV-2 genomes sequenced worldwide. To align these sequences, we used MAFFT (Katoh & Standley, 2013) plugin from Geneious Prime 2.1 (Kearse et al., 2012), eliminating 597 sequences with the highest number of differences and ambiguities relative to the reference sequence (RefSeq: NC_045512.2), for a total of 5,000 sequences. Next, we estimated the frequency of SNP variants using the Find Variations/SNPs tool with a minimum coverage of 4,900 sequences and a minimum frequency of 0.01, to identify nucleotide variants among a subset of high quality sequenced genomes in order to evaluate ongoing evolution in the regions under positive selection.

Analysis of RNA and Protein structures

To investigate potential structural changes in Nsp4 and Nsp16 at both the RNA and protein level, we performed minimum free energy (MFE) prediction analysis using the RNAfold WebServer

(Gruber et al., 2008; Lorenz et al., 2011) and consensus homology modeling using PHYRE2's intensive mode (Kelley et al., 2016). These analyses were performed for both Nsp4 and Nsp16 sequences for SARS-CoV-2, Bat-CoV_RaTG13, Pan-CoV-Guangdong, and SARS-CoV. RNAfold uses a loop-based energy model and a dynamic programming algorithm to predict the structure of the sequence such that the free energy of the structure is minimized. The RNAfold WebServer generates graphical outputs for both the MFE and Centroid structures, which display the base pairing probabilities by color (blue = 0, red = 1). These two MFE structures correspond to the MFE and the Centroid traces in the mountain plot, which is a positional representation of the secondary structure. In our figures, we show the MFE structure prediction.

PHYRE2 aligns input protein sequences using Position-Specific Iterated BLAST (PSI-BLAST) against sequences of experimentally resolved protein structures. A 3D model of the input sequence is then constructed based on homology-matched templates, optimizing for greatest sequence coverage and highest confidence. Regions of the input sequence without a matching template sequence are modeled *ab initio* and with Poing, a multi-template modelling tool. Pairwise comparisons of predicted protein structures were visualized using PyMOL software (DeLano, 2002). Alignment and structural comparisons performed by FATCAT (Ye & Godzik, 2004).

Results

Positive and negative selection are highly localized within coronavirus genomes

We tested for branch-specific selection on nucleotide sequences in coronavirus genomes, focusing on six species from the *Sarbecovirus* Subgenus (Coronaviridae family) and Bat-CoV-BM48-31/BGR/2008 as an outgroup. Using 300 bp windows with a step size of 150 bp, we scanned the genome alignment for concentrations of fixed mutations that exceed the neutral expectation based on the genome as whole relative to that particular window's evolutionary history among the seven species. This test identifies regions of the genome showing the most extreme divergence in nucleotide sequence on a particular branch relative to its specific background rate of evolution across the entire phylogeny and without reference to the genetic code. Fig 1A shows windows of inferred positive selection (red dots) on the branch leading to each species. The results reveal several signals of positive selection that are unique to a single species and others that are recapitulated in multiple species. The latter finding suggests that some segments of the viral genome have repeatedly experienced adaptive modification. In general, the

distribution of positive selection is more similar in closely related species than in divergent ones (Figs 1A and 1B), suggesting that some molecular functions have been altered over an interval that extends beyond the origin of a single species but not across the entire Sarbecovirus radiation.

Next, we identified regions of the genome that are highly conserved across the sarbecovirus genomes examined in this study using PhastCons (Siepel et al., 2005) (Fig 2A). As with positive selection, conservation is highly localized (Figs 2A and 2B). Based on a criterion of PhastCons > 0.9, we found high levels of conservation in regions encoding seven proteins: 3CL-Pro, Nsp6, Nsp8, Nsp9, Nsp10, Nsp11, RNA-dependent RNA polymerase (RdRp), Protein 3a, Nucleocapsid phosphoprotein, and Envelope (Figs 2A-D). These loci of exceptional sequence conservation highlight critical molecular features: Nucleocapsid and Envelope are essential structural proteins of the coronavirus capsid, while the other proteins regulate a variety of molecular process during viral replication (Tan et al., 2005; Lu et al., 2006; Minakshi et al., 2009; Freundt et al., 2010; Fuchs, 2012; Yue et al., 2018).

The gene encoding Spike protein is under persistent positive selection

In all ingroup species examined we detected signals of positive selection within the S gene, which encodes the Spike protein, and in five of the six species this was the most prominent signal in the entire genome (Fig 1A). This finding confirms previous studies that used the dN/dS ratio to test for selection on protein function (Tang et al., 2020; Chaw et al., 2020; Li et al., 2020a). Interestingly, we observed that the specific regions showing signatures of positive selection differed between species (Figs 1B and 1C). In SARS-CoV-2, we detected signals of positive selection in four segments of the S gene. First, the region encoding the entire receptor binding domain (RBD) shows an extended signal (Figs 1B-C and 3A); as others have noted, structural changes in this region may improve binding to human ACE2 (Wang et al., 2020; Wrapp et al., 2020; Wang, Liu & Gao, 2020). The second segment encodes another externally facing region, the S1 subunit N-terminal (NTD) domain, which includes the first disulfide bond (amino acids 13 - 113) and several glycosylation sites. The third signal of positive selection within S is located around the derived furin cleavage site (amino acids 664 - 812) that has been found to be essential for infection of lung cells (Hoffmann, Kleine-Weber & Pöhlmann, 2020). The fourth signal is located in a segment encoding the S2 and S2' subunits that includes the Heptad repeat 2 (amino acids 1114 - 1213). These heptad repeats were previously associated

with episodes of selection for amino acids that increase the stability of the six-helix bundle formed by both heptad repeats in MERS and other coronaviruses (Forni et al., 2015); they are also thought to determine host expansions and therefore, facilitate virus cross-species transmission (Graham & Baric, 2010).

The distribution of inferred positive selection in the S gene of SARS-CoV differed from that of SARS-CoV-2 described above. Notably, there was no signal in the ACE2 binding domain (Figs 1B and 1C). Moreover, a signal was present throughout the N-terminal domain and in the boundary region between the S1 and the S2 subunits (Fig 1), a region that includes the proteolytic cleavage (M de Haan et al., 2004). Interestingly, this region evolved a novel furin cleavage site in SARS-CoV-2 that may increase the cleavage efficiency and cell-cell fusion activity and changes in the virulence of the virion as seen in mutant studies of SARS-CoV and SARS-CoV-2 (Follis, York & Nunberg, 2006; Hoffmann, Kleine-Weber & Pöhlmann, 2020).

Genes encoding Nsp4 and Nsp16 contain branch-specific signals of positive selection

We also detected two shorter signals of positive selection within the SARS-CoV-2 genome that are located outside of the S gene, in ORF1a and ORF1b (Fig 1A). Interestingly, both encode small proteins that contribute to viral replication. The first is Nsp4, which encodes a membrane-bound protein with a cytoplasmic C-terminal domain; it is thought to anchor the Viral-Replication-Transcription Complex (RTC) to the modified endoplasmic reticulum membranes in the host cell (Oostra et al., 2008; Hagemeijer et al., 2011, 2014; Snijder, Decroly & Ziebuhr, 2016). The SARS-CoV-2 Nsp4 protein differs from that of closely related sarbecoviruses by two nearly adjacent amino acids: V380A and V382I. Although this region of the genome as a whole is not highly conserved (Fig 2), both of these positions are V residues in all of the in-group species we examined except SARS-CoV-2 (Fig 3B and 4A). This signal is too weak to be scored as positive selection using dN/dS-based tests (Sharp, 1997; Nielsen, 1997; Yang & Nielsen, 2008) and indeed may not affect protein function given the biochemically similar side-chains of the amino acids involved.

The second signal of positive selection outside of the S gene lies within Nsp16. This gene encodes a 2'-O-methyltransferase that modifies the 5'-cap of viral mRNAs (Decroly et al., 2008; Bouvet et al., 2010) and assists in evasion of the innate immune system of host cells (Züst et al., 2011; Menachery, Debbink & Baric, 2014; Nelemans & Kikkert, 2019). Of note, this is the only signal of positive selection within the SARS-CoV-2 genome that lacks any nonsynonymous

substitutions (Fig 2). All of the nucleotide substitutions in Nsp16 during the origin of SARS-CoV-2 are synonymous, while the Nsp16 genes of SARS-CoV-2, Bat-Cov-RaTG13, and Pan-CoV-GD (Guangdong) all encode identical proteins (Figs 3C and 5A). This suggests a complex mechanism of selection in the form of purifying selection at the protein level and positive selection at the nucleotide level. Ancestral state reconstruction of Nsp16 indicates that 20 synonymous substitutions likely occurred in the lineage leading to SARS-CoV-2 after the split from the common ancestor with BatCoV-RaTG13, while 19 substitutions are synonymous substitutions that occurred in the lineage leading to Bat-CoV-RaTG13 (Supplementary data). Eleven of these twenty substitutions are concentrated within the region scoring high for positive selection in SARS-CoV-2 and twelve within the positively selected region in Bat-CoV-RaTG13. Surprised by these findings, we hypothesized that the Nsp16 RNA secondary structure may differ among species in ways that affect molecular functions mediated directly (although not solely) by RNA, such as replication, transcription, translation, or evasion of the host immune system. To investigate this possibility, we first compared the secondary structure and minimum free energy (MFE) of RNA in the vicinity of Nsp4 and Nsp16 among the genomes of SARS-CoV-2, Bat-CoV-RaTG13, Pan-CoV-GD, and SARS-CoV using RNAfold (Gruber et al., 2008). Both the predicted secondary structures and mountain plots, which show the free energy predictions along the length of the sequence by position, reveal differences in RNA folding dynamics across the four species (Figs 4B and 5B). Analysis of the reconstructed sequence of the SARS-CoV-2 + Bat-CoV-RaTG13 ancestor reveal that most of these differences evolved during the origin of SARS-CoV-2 (S1 Fig). These differences among species in predicted secondary structures within Nsp4 and Nsp16 stand in contrast to the 5’ UTR, which is thought to fold into a stable secondary structure that is markedly conserved among Sarbecovirus species (S3 Fig). Together, these observations suggest that the signal of positive selection within Nsp16 in the SARS-CoV-2 genome may reflect changes in RNA, rather than protein, function that are unique to this species of coronavirus.

While the focus here is on SARS-CoV-2, it is worth noting that we also detected signals of positive selection outside of the S gene in the other sarbecovirus genomes examined here. The distribution of positive selection in the genome of SARS-CoV, for instance, shows some similarities to, but also notable differences from, that of SARS-Cov-2 (Fig 1). In both species, S and Nsp16 contain signals of positive selection, although in distinct regions of the two genes (Fig

1). In addition, the genome of SARS-CoV contains signals of positive selection in Nsp2, Nsp3, and ORF3a, none of which shows elevated rates of substitution in SARS-CoV-2. The first two genes encode proteins with important roles in viral replication: Nsp2 may disrupt intracellular signaling in the host cell (Cornillez-Ty et al., 2009) while Nsp3 cleaves itself, Nsp1, and Nsp2 from the replicase polyproteins (Báez-Santos, St. John & Mesecar, 2015), assists in the assembly of the double membrane vesicles of the RTC system (Hagemeijer et al., 2014), and antagonizes the host innate immune response (Tsuchida, Kawai & Akira, 2009; Frieman et al., 2009; Matthews et al., 2014).

Recombination does not account for most signals of positive selection

Recombination from another species can be a confounding factor in the inference of positive selection using the framework employed here, because the inserted genomic segment may be more divergent than the rest of the foreground genome is from nearby background species. Several instances of recombination have been reported in coronaviruses, including SARS-CoV-2 (Hon et al., 2008; Lam et al., 2020; Boni et al., 2020; Li et al., 2020a), making it important to distinguish regions of recombination from positive selection. The two processes produce distinct genetic signatures, with recombination the result of a single event (possibly later further recombined) and positive selection as detected here the result of multiple independent mutations that were fixed over an extended interval and are spatially concentrated. In order to test for regions of the SARS-CoV-2 that contain recombined segments from other species, we estimated the phylogenetic history of 500 bp segments of the genome with a step size of 150 bp among the aligned genomes of the seven species examined in this study. We used RaXML-NG v0.9 (Kozlov et al., 2019) to reconstruct topology for each segment independently and searched for cases where the topology differed from the expected topology based on the entire genome: (Bat-CoV-BM48, ((Bat-CoV-LYRa11, SARS-CoV), (Pa-CoV-GX, (Pa-CoV-GD, (SARS-CoV-2, Ba-CoV-RaTG13)))). Recombination from a divergent species should produce an incongruent topology in one or more adjacent windows, revealing a recombined region and its approximate breakpoints. We identified 12 regions where the topology differed from the expected (Fig 6). Of note, these regions are somewhat more concentrated in the part of the genome that encodes structural proteins. Consistent with a previous report (Li et al., 2020a), we observed overlap between regions scoring high for positive selection and recombination in S, the gene encoding Spike protein (Fig 6M), specifically the region that encodes for the ACE2 binding domain and a

region that includes the furin-cleavage site (Figs 6F-G). Importantly, however, none of the putatively recombined regions overlap with the windows scoring high for positive selection within the genes encoding Nsp4 and Nsp16 proteins in SARS-CoV-2.

Recent changes in allele frequency may result from positive selection and hitch-hiking

To gain insight into the evolutionary mechanisms that have shaped genetic variation more recently within the SARS-CoV-2 genome, we compiled a list of known mutations, based on 5,000 accessions sequenced since the beginning of the current pandemic (see Methods). As expected, the vast majority of variants are singletons, representing either mutations that are not segregating or sequencing errors. The density distribution of polymorphisms (regardless of frequency) is elevated within 2-3 kb at both ends the SARS-CoV-2 genome (Fig 2D). The site-frequency spectrum is strongly left-skewed (S2 Fig). Given that the effective population size of SARS-CoV-2 is likely very large, this distribution suggests that most SNPs are not subject to positive selection and that negative selection prevents most new mutations from rising in frequency due to drift. However, we did observe four SNPs that are present at high alternative allele frequency (AAF > 0.6) (Fig 2C), a situation that can reflect positive selection, drift, or hitch-hiking. Interestingly, all four of these SNPs are in tight LD (Toyoshima et al., 2020), which suggests that positive selection on one of them may have driven the other three to high frequency due to hitch-hiking.

We next investigated the likely consequences for altered molecular function due to each of these four high-frequency derived SNPs. Two are located within regions of the genome that are highly conserved among sarbecovirus species (Figs 2B-C). The first is a C>U substitution at position 241 in the 5'UTR, a region of the genome where RNA secondary structure is highly conserved across Coronavirus species (Madhugiri et al., 2016; Rangan et al., 2020; Alhatlani, 2020). Using RNAfold (Gruber et al., 2008) we found that this C>U transition had no impact on the stem-loop structure established for SARS-CoV (S3 Fig). The other mutation in a conserved region of the genome is a nonsynonymous substitution in the RdRp gene (14,408; P323L) at the interface domain, which is thought to mediate protein-protein interactions (Pachetti et al., 2020; Hillen et al., 2020). Because proline residues can influence secondary structure, we used PHYRE2 to predict the impact of the P232L mutation on protein structure. Comparison of the two predicted structures using FATCAT shows they are nearly identical (Table S1). The other two high-frequency derived SNPs are located in regions that are neither highly conserved nor highly

372 divergent. One is a synonymous SNP in Nsp3 (3,037) and the other a nonsynonymous SNP in S
373 (23,403; D614G). This last SNP effectively removes a charged side-chain between the receptor
374 binding domain and the furin cleavage site of S, a region of recurrent positive selection among
375 the Sarbecovirus species we examined. Thus, of the four high-frequency derived SNPs, the
376 nonsynonymous substitution in S the most plausible candidate for altering molecular function
377 and thus becoming a target of natural selection.
378

379 ## Discussion

380 A crucial feature contributing to the global spread of Covid19 is that viral shedding starts before
381 the onset of symptoms (He et al., 2020); in contrast, shedding began two to ten days after the
382 onset of symptoms during the SARS epidemic of 2003 (Peiris et al., 2003; Pitzer, Leung &
383 Lipsitch, 2007). This striking difference suggests that one or more molecular mechanisms during
384 host cell invasion, virus replication, or immune avoidance may have changed during the origin of
385 SARS-CoV-2. Mutations contributing to viral transmission would likely be favored by natural
386 selection, making tests for positive selection a useful tool for identifying candidate genetic
387 changes responsible for the unique properties of SARS-CoV-2. Here, we searched for regions of
388 possible positive selection within the genomes of six coronavirus species, including SARS-CoV
389 and SARS-CoV-2. The method we used tests for an excess of branch-specific nucleotide
390 substitutions within a defined window relative to a neutral expectation for divergence in that
391 window and without regard to the genetic code (Wong & Nielsen, 2004; Haygood et al., 2007;
392 Berrio, Haygood & Wray, 2020).
393 Several prior studies have identified *S*, the gene encoding the Spike glycoprotein, as a target of
394 recurrent positive selection in coronavirus genomes, including SARS-CoV-2, based on ω, the
395 ratio of synonymous to nonsynonymous substitutions (Andersen et al., 2020; Cagliani et al.,
396 2020; Tang et al., 2020; Armijos□Jaramillo et al., 2020; Lam et al., 2020; Li et al., 2020a). S
397 thus serves as a positive control for our ability to detect signals of positive selection using a
398 different approach, which uses a likelihood ratio framework to identify regions of elevated,
399 branch-specific nucleotide substitution rates relative to a model that allows only drift (Wong &
400 Nielsen, 2004; Haygood et al., 2007; Berrio, Haygood & Wray, 2020). Consistent with this
401 expectation, we found that portions of the gene encoding Spike showed a striking elevation of
402 sequence divergence relative to the rest of the genome on the branches leading to all six species

examined. The specific regions of S containing high divergence differs markedly, however, among species (Fig 1B). In SARS-CoV and Bat-CoV-LYRa11, these regions include the N-terminal region, which contains glycosylation sites important for viral camouflage (Watanabe et al., 2019; Yang et al., 2020) and a site of proteolytic cleavage that allows entry into the host cell (Belouzard, Chu & Whittaker, 2009) (Fig 1C and 3A). In contrast, signals of positive selection in SARS-CoV-2 and Bat-CoV-RaTG13 are concentrated in the domain that mediates binding to the host receptor ACE2 (Fig 1C and 3A). These distinct distributions suggest that modifications in different aspects of Spike function took place as various coronaviruses adapted to novel hosts. In particular, the concentration of derived amino acid substitutions in the receptor binding domain of Spike (Figs 1B and 1C) in SARS-CoV-2 and Bat-CoV-RaTG13 may reflect selection for amino acid substitutions that result in higher affinity for ACE2 protein in different host species. Importantly, we also detected signals of positive selection in two additional regions of the SARS-CoV-2 genome, specifically within the genes encoding Nsp4 and Nsp16 (Fig 1A). Of note, the Nsp16 region also shows a parallel signal of positive selection on the branch leading to SARS-CoV. To our knowledge, this is the first report of possible adaptive change in molecular function during the evolutionary origin of SARS-CoV-2 outside of the gene encoding Spike protein. Prior scans for positive selection within the SARS-CoV-2 genome used elevated ω as the signal of positive selection, which restricts attention to positive selection based on changes in protein function. For coronaviruses this is a notable limitation, given that many aspects of the lifecycle involve RNA function (Madhugiri et al., 2016; Ziv et al., 2020; Alhatlani, 2020). In addition, the secondary structure of some segments within the RNA genome is well conserved among coronavirus species, which implies a functional role (Rangan et al., 2020; Sanders et al., 2020; Huston et al., 2020a). Indeed, the SARS-CoV-2 genome is reported to contain more well-structured regions than any other known virus, including both coding and noncoding regions of the genome (Huston et al., 2020a). We therefore examined nucleotide substitutions within regions of putative positive selection in Nsp4 and Nsp16 for their likely impact on both protein and RNA structure (Fig 4 and 5).

In the case of Nsp4 protein, two nearly adjacent nonsynonymous substitutions at residues 380 and 382 occurred on the branch leading to SARS-CoV-2 (Fig 3B). These both involve changing side chains with similar biochemical properties, respectively valine to alanine and valine to isoleucine. Homology-directed modeling of protein structure suggests that these two amino acid

substitutions have very little impact on either secondary or tertiary structure when comparing the SARS-CoV-2 protein orthologue to those of the other species examined (Fig 4A). In the case of Nsp16 protein, no nonsynonymous substitutions evolved on the branch leading to SARS-CoV-2. Thus, the signal of positive selection within Nsp4 is unlikely to reflect changes in protein structure or function, while the signal within Nsp16 cannot affect either because the encoded polypeptide is identical.

With highly similar and identical protein structures predicted for Nsp4 and Nsp16, respectively, we considered the possibility that the signals of positive selection instead reflect changes in RNA structure and function. Previous studies found that neither the Nsp4 nor Nsp16 regions stand out as particularly well folded regions of the genome, although Nsp16 does contain a single well-folded region and Nsp4 two moderately well folded regions (Rangan et al., 2020; Huston et al., 2020b). Further, both genes show significantly decreased sequence divergence among coronavirus species within predicted double-stranded regions] (Rangan et al., 2020; Sanders et al., 2020; Huston et al., 2020a). Indeed, the well-folded region within Nsp16 is the only such region in the SARS-CoV-2 genome that is also well conserved among related coronaviruses (Sanders et al., 2020). These published observations suggest possible functional roles for folded structures within Nsp4 and Nsp16. Our minimum free energy (MFE) predictions reveal that the likely secondary structure of the RNA genome in the region of the Nsp4 and Nsp16 genes likely differs among the six coronavirus species we examined (Fig 4B and 5B, top rows). The MFE predictions also indicate differences among species in entropy across the regions containing the signals of positive selection, indicating likely differences in the stability of the folded molecule (Fig 4B and 5B, bottom rows). Together, these new results indicate that the folded regions of Nsp4 and Nsp16 in the SARS-Cov-2 genome may differ in shape from those of related coronaviruses.

Unfortunately, little is currently known about the molecular functions of secondary structures in coronavirus genomes. Most of the attention has been directed towards the 5' UTR, 3' UTR, and frameshift element at the junction between Orf1a and Orf1b, which together contain the most well-folded regions in the SARS-CoV-2 genome (Andrews et al., 2020; Sanders et al., 2020; Huston et al., 2020a). Thus, it is not possible at this time to link structural and thermodynamic features within Nsp4 and Nsp16 that are unique to SARS-CoV-2 to specific molecular functions. As discussed above, however, published evidence suggests that RNA secondary structures within

these regions of the genome may be functional (Rangan et al., 2020; Sanders et al., 2020; Huston et al., 2020a). These functions could, in principle, affect genome or transcript function, or both. Plausible possibilities include secondary structures that recruit specific RNA-binding proteins to mediate transcriptional regulation or transcript processing (Pirakitikulr et al., 2016; Pan et al., 2020), that mediate looping for other reasons (Gebhard, Filomatori & Gamarnik, 2011; Ziv et al., 2020), or that simply facilitate or impede processivity of the replication or translation machinery (MacFadden et al., 2018).

Conclusions

Scans for positive selection typically focus on changes in protein function and far less often consider the possibility of adaptive change in RNA function. By shining a light on regions of the SARS-CoV-2 genome that appear to be under positive selection yet are unlikely to alter protein function, our results illustrate the value of evaluating the potential for adaptive changes in secondary structures within the genomes of RNA viruses. In particular, we identify Nsp4 and Nsp16 as regions of the SARS-Cov-2 genome that may contain mutations that contribute to the unique biological and epidemiological features of this recently emerged pathogen.

While it is tempting to speculate about the possible adaptive role of changes in RNA structure within these accelerated regions, we suggest that this is best done in the context of relevant experimental results. For example, it might be informative to modify the primary sequence of the genome so as to encode the same protein sequence while altering or disrupting secondary structure within Nsp4 or Nsp16, then assay the consequences for viral replication and for specific molecular functions. We hope that our results inspire these or other experiments aimed at better understand the evolving functions of RNA secondary structure within the SARS-CoV-2 genome.

Acknowledgements

The authors would like to thank all the members of the lab groups of David McClay and Greg Wray for comments and the Compact for Open-Access Publishing Equity (COPE) program at Duke University for supporting publication costs.

References

Alhatlani BY. 2020. In silico identification of conserved cis -acting RNA elements in the SARS-CoV-2 genome. *Future Virology*:fvl-2020-0163. DOI: 10.2217/fvl-2020-0163.

Andersen KG, Rambaut A, Lipkin WI, Holmes EC, Garry RF. 2020. The proximal origin of SARS-CoV-2. *Nature Medicine* 26:450–452. DOI: 10.1038/s41591-020-0820-9.

Andrews RJ, Peterson JM, Haniff HS, Chen J, Williams C, Grefe M, Disney MD, Moss WN. 2020. An in silico map of the SARS-CoV-2 RNA Structurome. *bioRxiv : the preprint server for biology*:2020.04.17.045161. DOI: 10.1101/2020.04.17.045161.

Armijos Jaramillo V, Yeager J, Muslin C, Perez Castillo Y. 2020. SARS CoV 2, an evolutionary perspective of interaction with human ACE2 reveals undiscovered amino acids necessary for complex stability. *Evolutionary Applications*:eva.12980. DOI: 10.1111/eva.12980.

Báez-Santos YM, St. John SE, Mesecar AD. 2015. The SARS-coronavirus papain-like protease: Structure, function and inhibition by designed antiviral compounds. *Antiviral Research* 115:21–38. DOI: 10.1016/j.antiviral.2014.12.015.

Belouzard S, Chu VC, Whittaker GR. 2009. Activation of the SARS coronavirus spike protein via sequential proteolytic cleavage at two distinct sites. *Proceedings of the National Academy of Sciences of the United States of America* 106:5871–5876. DOI: 10.1073/pnas.0809524106.

Berrio A, Haygood R, Wray GA. 2020. Identifying branch-specific positive selection throughout the regulatory genome using an appropriate proxy neutral. *BMC Genomics* 21:359. DOI: 10.1186/s12864-020-6752-4.

Boni MF, Lemey P, Jiang X, Lam TT-Y, Perry BW, Castoe TA, Rambaut A, Robertson DL. 2020. Evolutionary origins of the SARS-CoV-2 sarbecovirus lineage responsible for the COVID-19 pandemic. *Nature Microbiology*:2020.03.30.015008. DOI: 10.1038/s41564-020-0771-4.

Bouvet M, Debarnot C, Imbert I, Selisko B, Snijder EJ. 2010. In Vitro Reconstitution of SARS-Coronavirus mRNA Cap Methylation. *PLoS Pathog* 6:1000863. DOI: 10.1371/journal.ppat.1000863.

Cagliani R, Forni D, Clerici M, Sironi M. 2020. Computational Inference of Selection Underlying the Evolution of the Novel Coronavirus, Severe Acute Respiratory Syndrome Coronavirus 2 Downloaded from. *jvi.asm.org 1 Journal of Virology* 94:411–431. DOI: 10.1128/JVI.00411-20.

Chaw S-M, Tai J-H, Chen S-L, Hsieh C-H, Chang S-Y, Yeh S-H, Yang W-S, Chen P-J, Wang

H-Y. 2020. The origin and underlying driving forces of the SARS-CoV-2 outbreak. *Journal of biomedical science* 27:73. DOI: 10.1186/s12929-020-00665-8.

Cornillez-Ty CT, Liao L, Yates Iii JR, Kuhn P, Buchmeier MJ. 2009. Severe Acute Respiratory Syndrome Coronavirus Nonstructural Protein 2 Interacts with a Host Protein Complex Involved in Mitochondrial Biogenesis and Intracellular Signaling. *JOURNAL OF VIROLOGY* 83:10314–10318. DOI: 10.1128/JVI.00842-09.

Decroly E, Imbert I, Coutard B, Bouvet M, Selisko B, Alvarez K, Gorbalenya AE, Snijder EJ, Canard B. 2008. Coronavirus Nonstructural Protein 16 Is a Cap-0 Binding Enzyme Possessing (Nucleoside-2′O)-Methyltransferase Activity. *Journal of Virology* 82:8071–8084. DOI: 10.1128/jvi.00407-08.

DeLano WL. 2002. Pymol: An open-source molecular graphics tool. :40, 82–92.

Eaaswarkhanth M, Al Madhoun A, Al-Mulla F. 2020. Could the D614G substitution in the SARS-CoV-2 spike (S) protein be associated with higher COVID-19 mortality? *International journal of infectious diseases□: IJID□: official publication of the International Society for Infectious Diseases* 96:459–460. DOI: 10.1016/j.ijid.2020.05.071.

Fehr AR, Perlman S. 2015. Coronaviruses: An overview of their replication and pathogenesis. In: *Coronaviruses: Methods and Protocols*. Springer New York, 1–23. DOI: 10.1007/978-1-4939-2438-7_1.

Follis KE, York J, Nunberg JH. 2006. Furin cleavage of the SARS coronavirus spike glycoprotein enhances cell-cell fusion but does not affect virion entry. *Virology* 350:358–369. DOI: 10.1016/j.virol.2006.02.003.

Forni D, Filippi G, Cagliani R, De Gioia L, Pozzoli U, Al-Daghri N, Clerici M, Sironi M. 2015. The heptad repeat region is a major selection target in MERS-CoV and related coronaviruses. *Scientific Reports* 5:1–10. DOI: 10.1038/srep14480.

Freundt EC, Yu L, Goldsmith CS, Welsh S, Cheng A, Yount B, Liu W, Frieman MB, Buchholz UJ, Screaton GR, Lippincott-Schwartz J, Zaki SR, Xu X-N, Baric RS, Subbarao K, Lenardo MJ. 2010. The Open Reading Frame 3a Protein of Severe Acute Respiratory Syndrome-Associated Coronavirus Promotes Membrane Rearrangement and Cell Death. *Journal of Virology* 84:1097–1109. DOI: 10.1128/jvi.01662-09.

Frieman M, Ratia K, Johnston RE, Mesecar AD, Baric RS. 2009. Severe acute respiratory syndrome coronavirus papain-like protease ubiquitin-like domain and catalytic domain

regulate antagonism of IRF3 and NF-kappaB signaling. *Journal of virology* 83:6689–705. DOI: 10.1128/JVI.02220-08.

Fuchs SY. 2012. Ubiquitination-mediated regulation of interferon responses. *Growth Factors* 30:141–148. DOI: 10.3109/08977194.2012.669382.

Gallagher TM, Buchmeier MJ. 2001. Coronavirus Spike Proteins in Viral Entry and Pathogenesis. *Virology* 279:371–374. DOI: 10.1006/viro.2000.0757.

Gebhard LG, Filomatori C V., Gamarnik A V. 2011. Functional RNA elements in the dengue virus genome. *Viruses* 3:1739–1756. DOI: 10.3390/v3091739.

Graham RL, Baric RS. 2010. Recombination, reservoirs, and the modular spike: mechanisms of coronavirus cross-species transmission. *Journal of virology* 84:3134–46. DOI: 10.1128/JVI.01394-09.

Gruber AR, Lorenz R, Bernhart SH, Neuböck R, Hofacker IL. 2008. The Vienna RNA websuite. *Nucleic acids research* 36:70–74. DOI: 10.1093/nar/gkn188.

Hagemeijer MC, Monastyrska I, Griffith J, van der Sluijs P, Voortman J, van Bergen en Henegouwen PM, Vonk AM, Rottier PJM, Reggiori F, de Haan CAM. 2014. Membrane rearrangements mediated by coronavirus nonstructural proteins 3 and 4. *Virology* 458–459:125–135. DOI: 10.1016/j.virol.2014.04.027.

Hagemeijer MC, Ulasli M, Vonk AM, Reggiori F, Rottier PJM, de Haan CAM. 2011. Mobility and Interactions of Coronavirus Nonstructural Protein 4. *Journal of Virology* 85:4572–4577. DOI: 10.1128/JVI.00042-11.

Hahne F, Ivanek R. 2016. Visualizing genomic data using Gviz and bioconductor. In: *Methods in Molecular Biology*. Humana Press Inc., 335–351. DOI: 10.1007/978-1-4939-3578-9_16.

Haygood R, Fedrigo O, Hanson B, Yokoyama K-D, Wray GA. 2007. Promoter regions of many neural- and nutrition-related genes have experienced positive selection during human evolution. *Nature genetics* 39:1140–4. DOI: 10.1038/ng2104.

He X, Lau EHY, Wu P, Deng X, Wang J, Hao X, Lau YC, Wong JY, Guan Y, Tan X, Mo X, Chen Y, Liao B, Chen W, Hu F, Zhang Q, Zhong M, Wu Y, Zhao L, Zhang F, Cowling BJ, Li F, Leung GM. 2020. Temporal dynamics in viral shedding and transmissibility of COVID-19. *Nature Medicine* 26:672–675. DOI: 10.1038/s41591-020-0869-5.

Hillen HS, Kokic G, Farnung L, Dienemann C, Tegunov D, Cramer P. 2020. Structure of replicating SARS-CoV-2 polymerase. *Nature*. DOI: 10.1038/s41586-020-2368-8.

588 Hoffmann M, Kleine-Weber H, Pöhlmann S. 2020. A Multibasic Cleavage Site in the Spike
589 Protein of SARS-CoV-2 Is Essential for Infection of Human Lung Cells. *Molecular Cell*
590 78:779-784.e5. DOI: 10.1016/j.molcel.2020.04.022.
591 Hon C-C, Lam T-Y, Shi Z-L, Drummond AJ, Yip C-W, Zeng F, Lam P-Y, Chi F, Leung C.
592 2008. Evidence of the Recombinant Origin of a Bat Severe Acute Respiratory Syndrome
593 (SARS)-Like Coronavirus and Its Implications on the Direct Ancestor of SARS
594 Coronavirus. *JOURNAL OF VIROLOGY* 82:1819–1826. DOI: 10.1128/JVI.01926-07.
595 Hu B, Zeng L-P, Yang X-L, Ge X-Y, Zhang W, Li B, Xie J-Z, Shen X-R, Zhang Y-Z, Wang N,
596 Luo D-S, Zheng X-S, Wang M-N, Daszak P, Wang L-F, Cui J, Shi Z-L. 2017. Discovery of
597 a rich gene pool of bat SARS-related coronaviruses provides new insights into the origin of
598 SARS coronavirus. *PLOS Pathogens* 13:e1006698. DOI: 10.1371/journal.ppat.1006698.
599 Hubisz MJ, Pollard KS, Siepel A. 2011. PHAST and RPHAST: phylogenetic analysis with
600 space/time models. *Briefings in bioinformatics* 12:41–51. DOI: 10.1093/bib/bbq072.
601 Hulswit RJG, de Haan CAM, Bosch BJ. 2016. Coronavirus Spike Protein and Tropism Changes.
602 In: *Advances in Virus Research*. Academic Press Inc., 29–57. DOI:
603 10.1016/bs.aivir.2016.08.004.
604 Huston NC, Wan H, Araujo Tavares R de C, Wilen C, Pyle AM. 2020a. Comprehensive in-vivo
605 secondary structure of the SARS-CoV-2 genome reveals novel regulatory motifs and
606 mechanisms. *bioRxiv : the preprint server for biology*:1–46. DOI:
607 10.1101/2020.07.10.197079.
608 Huston NC, Wan H, Araujo Tavares R de C, Wilen C, Pyle AM. 2020b. Comprehensive in-vivo
609 secondary structure of the SARS-CoV-2 genome reveals novel regulatory motifs and
610 mechanisms. *bioRxiv : the preprint server for biology*:1–46. DOI:
611 10.1101/2020.07.10.197079.
612 Katoh K, Standley DM. 2013. MAFFT Multiple Sequence Alignment Software Version 7:
613 Improvements in Performance and Usability. *Molecular Biology and Evolution* 30:772–780.
614 DOI: 10.1093/molbev/mst010.
615 Kearse M, Moir R, Wilson A, Stones-Havas S, Cheung M, Sturrock S, Buxton S, Cooper A,
616 Markowitz S, Duran C, Thierer T, Ashton B, Meintjes P, Drummond A. 2012. Geneious
617 Basic: an integrated and extendable desktop software platform for the organization and
618 analysis of sequence data. *Bioinformatics (Oxford, England)* 28:1647–9. DOI:

10.1093/bioinformatics/bts199.

Kelley LA, Mezulis S, Yates CM, Wass MN, Sternberg MJE. 2016. The Phyre2 web portal for protein modeling, prediction and analysis. *Nature Protocols* 10:845–858. DOI: 10.1038/nprot.2015.053.

Kim D, Lee J-Y, Yang J-S, Kim JW, Kim VN, Chang H. 2020. The Architecture of SARS-CoV-2 Transcriptome. *Cell* 181:914-921.e10. DOI: 10.1016/j.cell.2020.04.011.

Korber B, Fischer WM, Gnanakaran S, Yoon H, Theiler J, Abfalterer W, Hengartner N, Giorgi EE, Bhattacharya T, Foley B, Hastie KM, Parker MD, Partridge DG, Evans CM, Freeman TM, de Silva TI, Sheffield COVID-19 Genomics Group, McDanal C, Perez LG, Tang H, Moon-Walker A, Whelan SP, LaBranche CC, Saphire EO, Montefiori DC. 2020. Tracking Changes in SARS-CoV-2 Spike: Evidence that D614G Increases Infectivity of the COVID-19 Virus. *Cell*. DOI: 10.1016/j.cell.2020.06.043.

Kozlov AM, Darriba D, Flouri T, Morel B, Stamatakis A, Wren J. 2019. RAxML-NG: A fast, scalable and user-friendly tool for maximum likelihood phylogenetic inference. *Bioinformatics* 35:4453–4455. DOI: 10.1093/bioinformatics/btz305.

Lam TT-Y, Jia N, Zhang Y-W, Shum MH-H, Jiang J-F, Zhu H-C, Tong Y-G, Shi Y-X, Ni X-B, Liao Y-S, Li W-J, Jiang B-G, Wei W, Yuan T-T, Zheng K, Cui X-M, Li J, Pei G-Q, Qiang X, Cheung WY-M, Li L-F, Sun F-F, Qin S, Huang J-C, Leung GM, Holmes EC, Hu Y-L, Guan Y, Cao W-C. 2020. Identifying SARS-CoV-2-related coronaviruses in Malayan pangolins. *Nature* 583:282–285. DOI: 10.1038/s41586-020-2169-0.

Lau SKP, Feng Y, Chen H, Luk HKH, Yang W-H, Li KSM, Zhang Y-Z, Huang Y, Song Z-Z, Chow W-N, Fan RYY, Ahmed SS, Yeung HC, Lam CSF, Cai J-P, Wong SSY, Chan JFW, Yuen K-Y, Zhang H-L, Woo PCY. 2015. Severe Acute Respiratory Syndrome (SARS) Coronavirus ORF8 Protein Is Acquired from SARS-Related Coronavirus from Greater Horseshoe Bats through Recombination. *Journal of Virology* 89:10532–10547. DOI: 10.1128/jvi.01048-15.

Li X, Giorgi EE, Marichannegowda MH, Foley B, Xiao C, Kong X-P, Chen Y, Gnanakaran S, Korber B, Gao F. 2020a. Emergence of SARS-CoV-2 through recombination and strong purifying selection. *Science Advances* 6:eabb9153. DOI: 10.1126/sciadv.abb9153.

Li Y, Yang X, Wang N, Wang H, Yin B, Yang X, Jiang W. 2020b. The divergence between SARS-CoV-2 and RaTG13 might be overestimated due to the extensive RNA modification.

Future Virology:fvl-2020-0066. DOI: 10.2217/fvl-2020-0066.

Liu P, Chen W, Chen J-P. 2019. Viral Metagenomics Revealed Sendai Virus and Coronavirus Infection of Malayan Pangolins (Manis javanica). *Viruses* 11:979. DOI: 10.3390/v11110979.

Lorenz R, Bernhart SH, Höner zu Siederdissen C, Tafer H, Flamm C, Stadler PF, Hofacker IL. 2011. ViennaRNA Package 2.0. *Algorithms for Molecular Biology* 6:26. DOI: 10.1186/1748-7188-6-26.

Lu W, Zheng BJ, Xu K, Schwarz W, Du L, Wong CKL, Chen J, Duan S, Deubel V, Sun B. 2006. Severe acute respiratory syndrome-associated coronavirus 3a protein forms an ion channel and modulates virus release. *Proceedings of the National Academy of Sciences of the United States of America* 103:12540–12545. DOI: 10.1073/pnas.0605402103.

M de Haan CA, Stadler K, Godeke G-J, Jan Bosch B, M Rottier PJ. 2004. Cleavage Inhibition of the Murine Coronavirus Spike Protein by a Furin-Like Enzyme Affects Cell-Cell but Not Virus-Cell Fusion Downloaded from. *JOURNAL OF VIROLOGY* 78:6048–6054. DOI: 10.1128/JVI.78.11.6048-6054.2004.

MacFadden A, Òdonoghue Z, Silva PAGC, Chapman EG, Olsthoorn RC, Sterken MG, Pijlman GP, Bredenbeek PJ, Kieft JS. 2018. Mechanism and structural diversity of exoribonuclease-resistant RNA structures in flaviviral RNAs. *Nature Communications* 9:1–11. DOI: 10.1038/s41467-017-02604-y.

Madhugiri R, Fricke M, Marz M, Ziebuhr J. 2016. Coronavirus cis-Acting RNA Elements. In: *Advances in Virus Research*. Academic Press Inc., 127–163. DOI: 10.1016/bs.aivir.2016.08.007.

Matthews K, Schäfer A, Pham A, Frieman M. 2014. The SARS coronavirus papain like protease can inhibit IRF3 at a post activation step that requires deubiquitination activity. *Virology Journal* 11:209. DOI: 10.1186/s12985-014-0209-9.

Menachery VD, Debbink K, Baric RS. 2014. Coronavirus non-structural protein 16: Evasion, attenuation, and possible treatments. *Virus Research* 194:191–199. DOI: 10.1016/j.virusres.2014.09.009.

Minakshi R, Padhan K, Rani M, Khan N, Ahmad F, Jameel S. 2009. The SARS Coronavirus 3a protein causes endoplasmic reticulum stress and induces ligand-independent downregulation of the type 1 interferon receptor. *PloS one* 4:e8342. DOI:

10.1371/journal.pone.0008342.

Nelemans T, Kikkert M. 2019. Viral innate immune evasion and the pathogenesis of emerging RNA virus infections. *Viruses* 11. DOI: 10.3390/v11100961.

Nielsen R. 1997. The ratio of replacement to silent divergence and tests of neutrality. *Journal of Evolutionary Biology* 10:217–231. DOI: 10.1046/j.1420-9101.1997.10020217.x.

Oostra M, Hagemeijer MC, van Gent M, Bekker CPJ, te Lintelo EG, Rottier PJM, de Haan CAM. 2008. Topology and Membrane Anchoring of the Coronavirus Replication Complex: Not All Hydrophobic Domains of nsp3 and nsp6 Are Membrane Spanning. *Journal of Virology* 82:12392–12405. DOI: 10.1128/jvi.01219-08.

Pachetti M, Marini B, Benedetti F, Giudici F, Mauro E, Storici P, Masciovecchio C, Angeletti S, Ciccozzi M, Gallo RC, Zella D, Ippodrino R. 2020. Emerging SARS-CoV-2 mutation hot spots include a novel RNA-dependent-RNA polymerase variant. *Journal of Translational Medicine* 18:1–9. DOI: 10.1186/s12967-020-02344-6.

Pan J, Qian X, Lattmann S, El Sahili A, Yeo TH, Jia H, Cressey T, Ludeke B, Noton S, Kalocsay M, Fearns R, Lescar J. 2020. Structure of the human metapneumovirus polymerase phosphoprotein complex. *Nature* 577:275–279. DOI: 10.1038/s41586-019-1759-1.

Peiris JSM, Chu CM, Cheng VCC, Chan KS, Hung IFN, Poon LLM, Law KI, Tang BSF, Hon TYW, Chan CS, Chan KH, Ng JSC, Zheng BJ, Ng WL, Lai RWM, Guan Y, Yuen KY. 2003. Clinical progression and viral load in a community outbreak of coronavirus-associated SARS pneumonia: A prospective study. *Lancet* 361:1767–1772. DOI: 10.1016/S0140-6736(03)13412-5.

Pirakitikulr N, Kohlway A, Lindenbach BD, Pyle AM. 2016. The Coding Region of the HCV Genome Contains a Network of Regulatory RNA Structures. *Molecular cell* 62:111–20. DOI: 10.1016/j.molcel.2016.01.024.

Pitzer VE, Leung GM, Lipsitch M. 2007. Estimating variability in the transmission of severe acute respiratory syndrome to household contacts in Hong Kong, China. *American Journal of Epidemiology* 166:355–363. DOI: 10.1093/aje/kwm082.

Pond SLK, Frost SDW, Muse S V. 2005. HyPhy: hypothesis testing using phylogenies. *Bioinformatics (Oxford, England)* 21:676–9. DOI: 10.1093/bioinformatics/bti079.

Pond SLK, Poon AFY, Velazquez R, Weaver S, Hepler NL, Murrell B, Shank SD, Magalis BR, Bouvier D, Nekrutenko A, Wisotsky S, Spielman SJ, Frost SDW, Muse S V. 2020. HyPhy

2.5-A Customizable Platform for Evolutionary Hypothesis Testing Using Phylogenies. *Molecular biology and evolution* 37:295–299. DOI: 10.1093/molbev/msz197.

Rangan R, Zheludev IN, Hagey RJ, Pham EA, Wayment-Steele HK, Glenn JS, Das R. 2020. RNA genome conservation and secondary structure in SARS-CoV-2 and SARS-related viruses: a first look. *RNA (New York, N.Y.)* 26:937–959. DOI: 10.1261/rna.076141.120.

Sanders W, Fritch EJ, Madden EA, Graham RL, Vincent HA, Heise MT, Baric RS, Moorman NJ. 2020. Comparative analysis of coronavirus genomic RNA structure reveals conservation in SARS-like coronaviruses. *bioRxiv : the preprint server for biology*. DOI: 10.1101/2020.06.15.153197.

Sharp PM. 1997. In search of molecular darwinism. *Nature* 385:111–112. DOI: 10.1038/385111a0.

Siepel A, Bejerano G, Pedersen JS, Hinrichs AS, Hou M, Rosenbloom K, Clawson H, Spieth J, Hillier LDW, Richards S, Weinstock GM, Wilson RK, Gibbs RA, Kent WJ, Miller W, Haussler D. 2005. Evolutionarily conserved elements in vertebrate, insect, worm, and yeast genomes. *Genome Research* 15:1034–1050. DOI: 10.1101/gr.3715005.

Snijder EJ, Decroly E, Ziebuhr J. 2016. The Nonstructural Proteins Directing Coronavirus RNA Synthesis and Processing. In: *Advances in Virus Research*. Academic Press Inc., 59–126. DOI: 10.1016/bs.aivir.2016.08.008.

Tan Y-J, Tham P-Y, Chan DZL, Chou C-F, Shen S, Fielding BC, Tan THP, Lim SG, Hong W. 2005. The Severe Acute Respiratory Syndrome Coronavirus 3a Protein Up-Regulates Expression of Fibrinogen in Lung Epithelial Cells. *Journal of Virology* 79:10083–10087. DOI: 10.1128/jvi.79.15.10083-10087.2005.

Tang X, Wu C, Li X, Song Y, Yao X, Wu X, Duan Y, Zhang H, Wang Y, Qian Z, Cui J, Lu J. 2020. On the origin and continuing evolution of SARS-CoV-2. *National Science Review* 7:1012–1023. DOI: 10.1093/nsr/nwaa036.

Tortorici MA, Veesler D. 2019. Structural insights into coronavirus entry. *Advances in virus research* 105:93–116. DOI: 10.1016/bs.aivir.2019.08.002.

Toyoshima Y, Nemoto K, Matsumoto S, Nakamura Y, Kiyotani K. 2020. SARS-CoV-2 genomic variations associated with mortality rate of COVID-19. *Journal of Human Genetics*:1–8. DOI: 10.1038/s10038-020-0808-9.

Tsuchida T, Kawai T, Akira S. 2009. Inhibition of IRF3-dependent antiviral responses by

743 cellular and viral proteins. *Cell Research* 19:3–4. DOI: 10.1038/cr.2009.1.
744 Velazquez-Salinas L, Zarate S, Eberl S, Gladue DP, Novella I, Borca M V. 2020. Positive
745 selection of ORF3a and ORF8 genes drives the evolution of SARS-CoV-2 during the 2020
746 COVID-19 pandemic. *bioRxiv*:2020.04.10.035964. DOI: 10.1101/2020.04.10.035964.
747 Wang Y, Liu M, Gao J. 2020. Enhanced receptor binding of SARS-CoV-2 through networks of
748 hydrogen-bonding and hydrophobic interactions. *Proceedings of the National Academy of*
749 *Sciences of the United States of America* 117:13967–13974. DOI:
750 10.1073/pnas.2008209117.
751 Wang Q, Zhang Y, Wu L, Niu S, Song C, Zhang Z, Lu G, Qiao C, Hu Y, Yuen KY, Wang Q,
752 Zhou H, Yan J, Qi J. 2020. Structural and Functional Basis of SARS-CoV-2 Entry by Using
753 Human ACE2. *Cell* 181:894-904.e9. DOI: 10.1016/j.cell.2020.03.045.
754 Watanabe Y, Bowden TA, Wilson IA, Crispin M. 2019. Exploitation of glycosylation in
755 enveloped virus pathobiology. *Biochimica et biophysica acta. General subjects* 1863:1480–
756 1497. DOI: 10.1016/j.bbagen.2019.05.012.
757 Wong WSW, Nielsen R. 2004. Detecting selection in noncoding regions of nucleotide
758 sequences. *Genetics* 167:949–58. DOI: 10.1534/genetics.102.010959.
759 Wrapp D, Wang N, Corbett KS, Goldsmith JA, Hsieh C-L, Abiona O, Graham BS, McLellan JS.
760 2020. Cryo-EM structure of the 2019-nCoV spike in the prefusion conformation. *Science*
761 367:1260–1263. DOI: 10.1126/science.abb2507.
762 Yang T-J, Chang Y-C, Ko T-P, Draczkowski P, Chien Y-C, Chang Y-C, Wu K-P, Khoo K-H,
763 Chang H-W, Hsu S-TD. 2020. Cryo-EM analysis of a feline coronavirus spike protein
764 reveals a unique structure and camouflaging glycans. *Proceedings of the National Academy*
765 *of Sciences* 117:1438–1446. DOI: 10.1073/pnas.1908898117.
766 Yang Z, Nielsen R. 2008. Mutation-selection models of codon substitution and their use to
767 estimate selective strengths on codon usage. *Molecular Biology and Evolution* 25:568–579.
768 DOI: 10.1093/molbev/msm284.
769 Ye Y, Godzik A. 2004. FATCAT: a web server for flexible structure comparison and structure
770 similarity searching. *Nucleic Acids Research* 32:W582–W585. DOI: 10.1093/nar/gkh430.
771 Yue Y, Nabar NR, Shi CS, Kamenyeva O, Xiao X, Hwang IY, Wang M, Kehrl JH. 2018. SARS-
772 Coronavirus Open Reading Frame-3a drives multimodal necrotic cell death. *Cell Death and*
773 *Disease* 9:1–15. DOI: 10.1038/s41419-018-0917-y.

774 Ziv O, Price J, Shalamova L, Kamenova T, Goodfellow I, Weber F, Miska EA. 2020. The short-
775 and long-range RNA-RNA Interactome of SARS-CoV-2 Co-first authors.
776 *bioRxiv*:2020.07.19.211110. DOI: 10.1101/2020.07.19.211110.
777 Züst R, Cervantes-Barragan L, Habjan M, Maier R, Neuman BW, Ziebuhr J, Szretter KJ, Baker
778 SC, Barchet W, Diamond MS, Siddell SG, Ludewig B, Thiel V. 2011. Ribose 2'-O-
779 methylation provides a molecular signature for the distinction of self and non-self mRNA
780 dependent on the RNA sensor Mda5. *Nature immunology* 12:137–43. DOI:
781 10.1038/ni.1979.
782

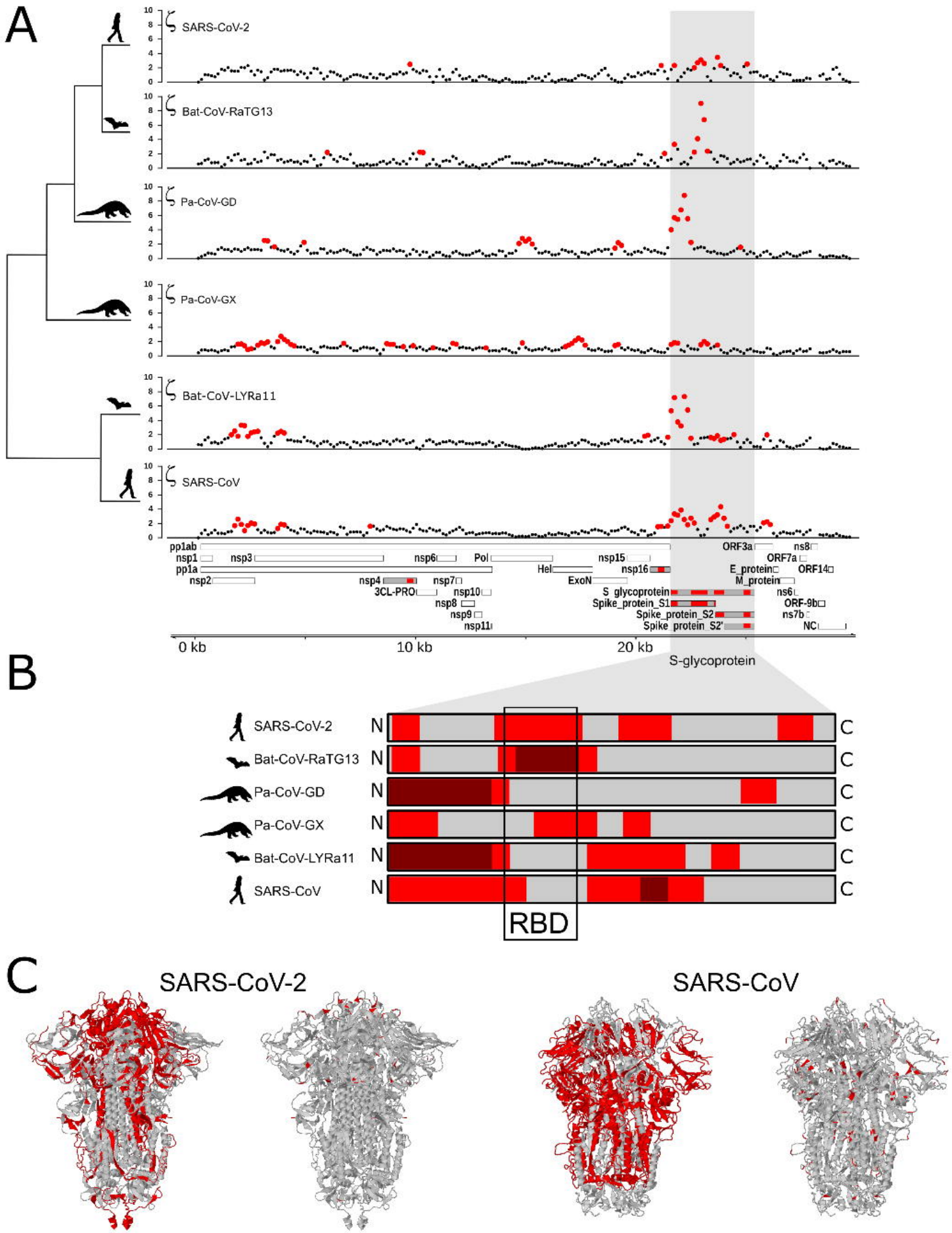
A
SARS-CoV-2
Bat-CoV-RaTG13
Pa-CoV-GD
Pa-CoV-GX
Bat-CoV-LYRa11
SARS-CoV
pp1ab
nsp1
nsp3
nsp6
Pol
nsp15
ORF3a
ns8
pp1a
Hel
nsp16
ORF7a
nsp2
ExoN
E_protein
ORF14
nsp4
nsp7
M_protein
3CL-PRO
nsp10
S_glycoprotein
ns6
nsp8
Spike_protein_S1
ORF-9b
nsp9
Spike_protein_S2
ns7b
nsp11
Spike_protein_S2'
NC
0 kb
10 kb
20 kb
S-glycoprotein
B
SARS-CoV-2
Bat-CoV-RaTG13
Pa-CoV-GD
Pa-CoV-GX
Bat-CoV-LYRa11
SARS-CoV
N
C
RBD
C
SARS-CoV-2
SARS-CoV

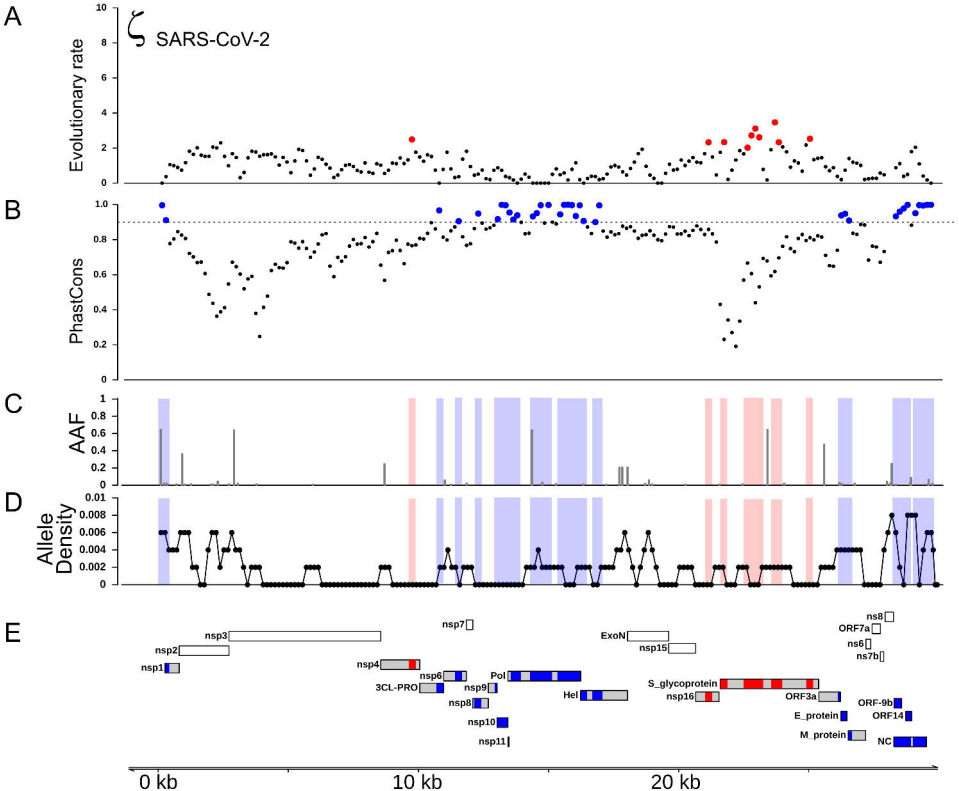
A
ζ SARS-CoV-2
Evolutionary rate
10
8
6
4
2
0
B
PhastCons
1.0
0.8
0.6
0.4
0.2
0
C
AAF
1
0.8
0.6
0.4
0.2
0
D
Allele Density
0.01
0.008
0.006
0.004
0.002
0
E
nsp1
nsp2
nsp3
nsp4
nsp6
3CL-PRO
nsp7
nsp8
nsp9
nsp10
nsp11
Pol
Hel
ExoN
nsp15
S_glycoprotein
nsp16
ns8
ORF7a
ns6
ns7b
ORF3a
E_protein
M_protein
ORF-9b
ORF14
NC
0 kb
10 kb
20 kb

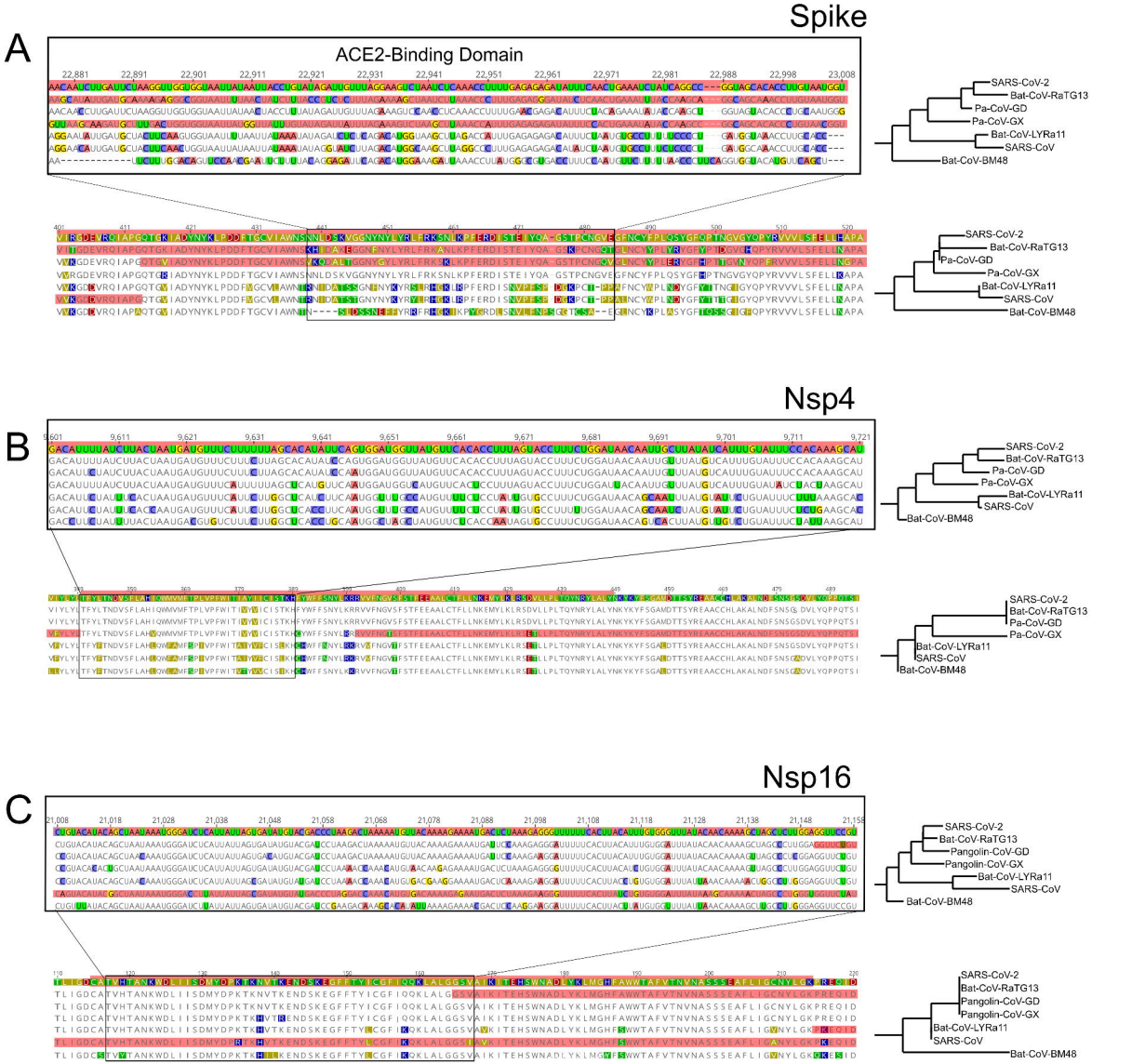
Spike
A
ACE2-Binding Domain
SARS-CoV-2
Bat-CoV-RaTG13
Pa-CoV-GD
Pa-CoV-GX
Bat-CoV-LYRa11
SARS-CoV
Bat-CoV-BM48
Nsp4
B
SARS-CoV-2
Bat-CoV-RaTG13
Pa-CoV-GD
Pa-CoV-GX
Bat-CoV-LYRa11
SARS-CoV
Bat-CoV-BM48
Nsp16
C
SARS-CoV-2
Bat-CoV-RaTG13
Pangolin-CoV-GD
Pangolin-CoV-GX
Bat-CoV-LYRa11
SARS-CoV
Bat-CoV-BM48

A

SARS-CoV-2

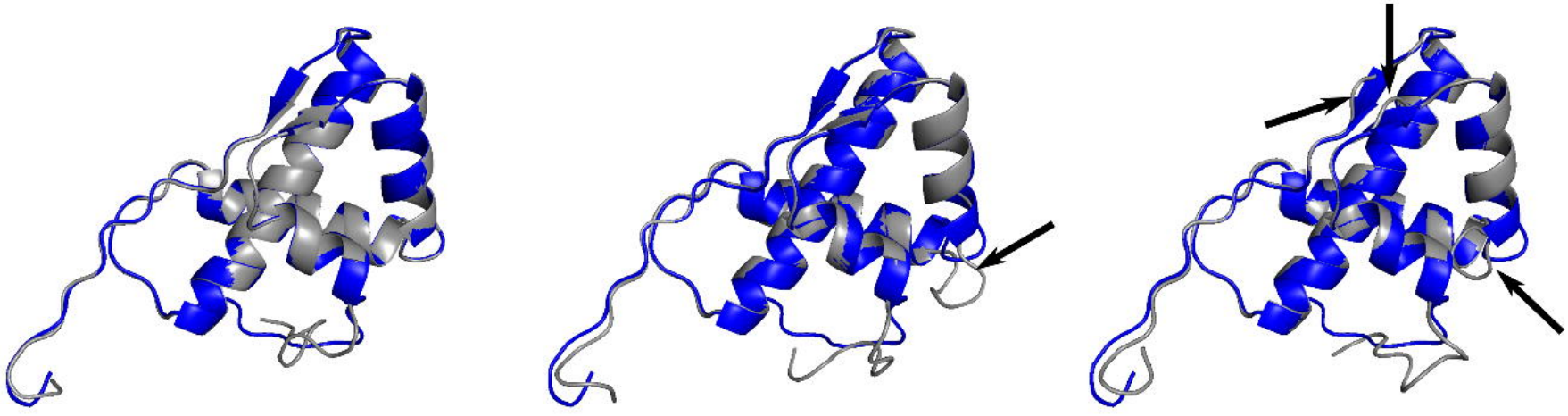

Bat-CoV-RaTG13 Pa-CoV-GD SARS-CoV

B

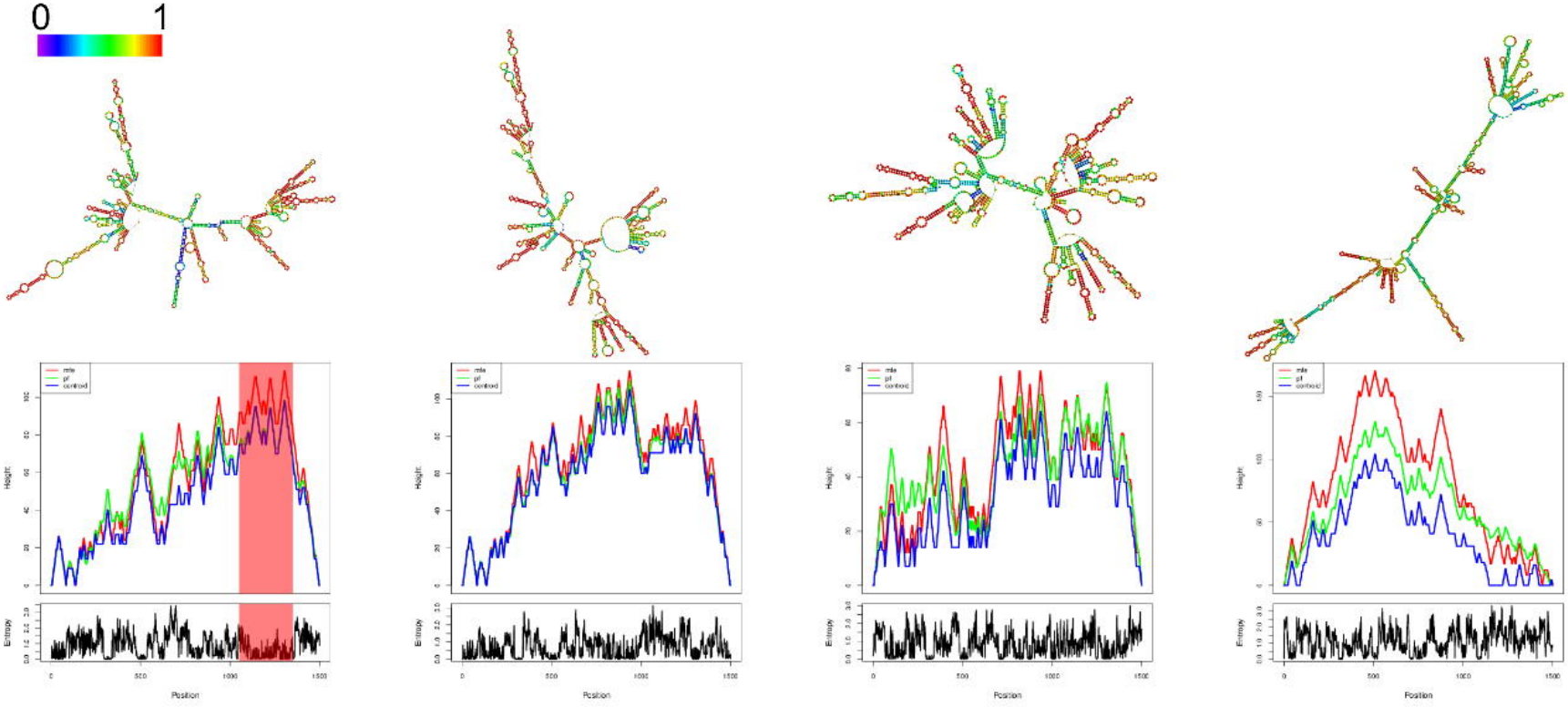

SARS-CoV-2 Bat-CoV-RaTG13 Pa-CoV-GD SARS-CoV

A

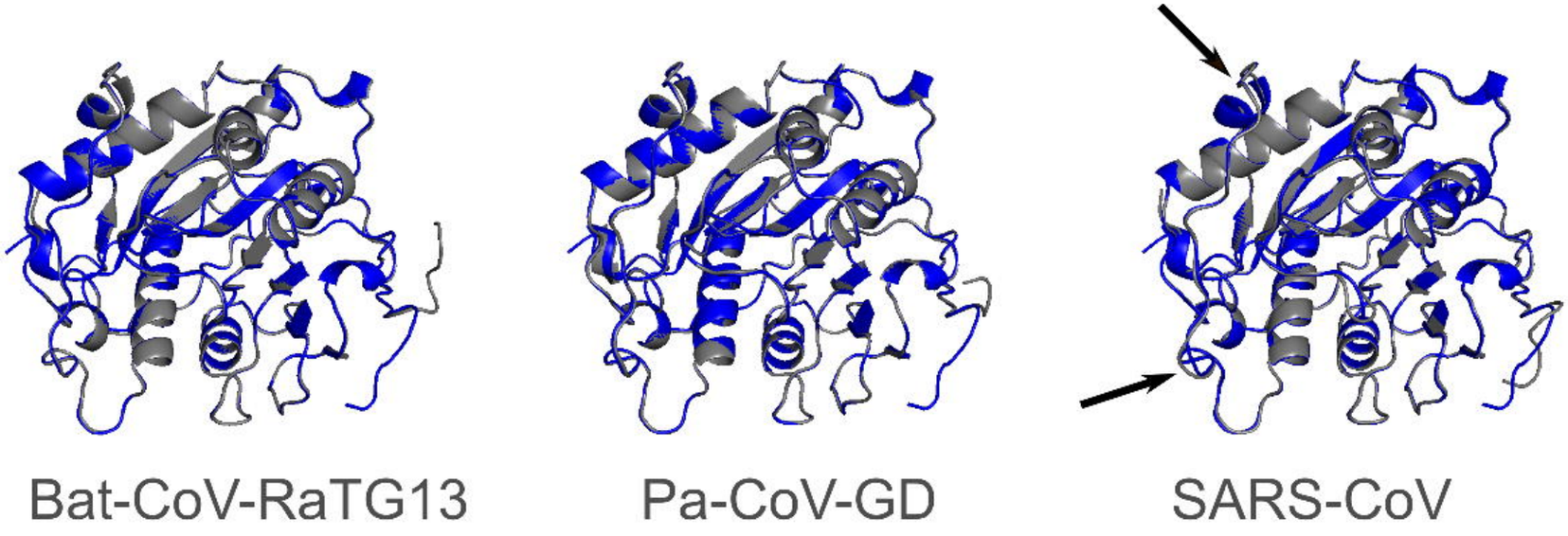
SARS-CoV-2
Bat-CoV-RaTG13
Pa-CoV-GD
SARS-CoV

B

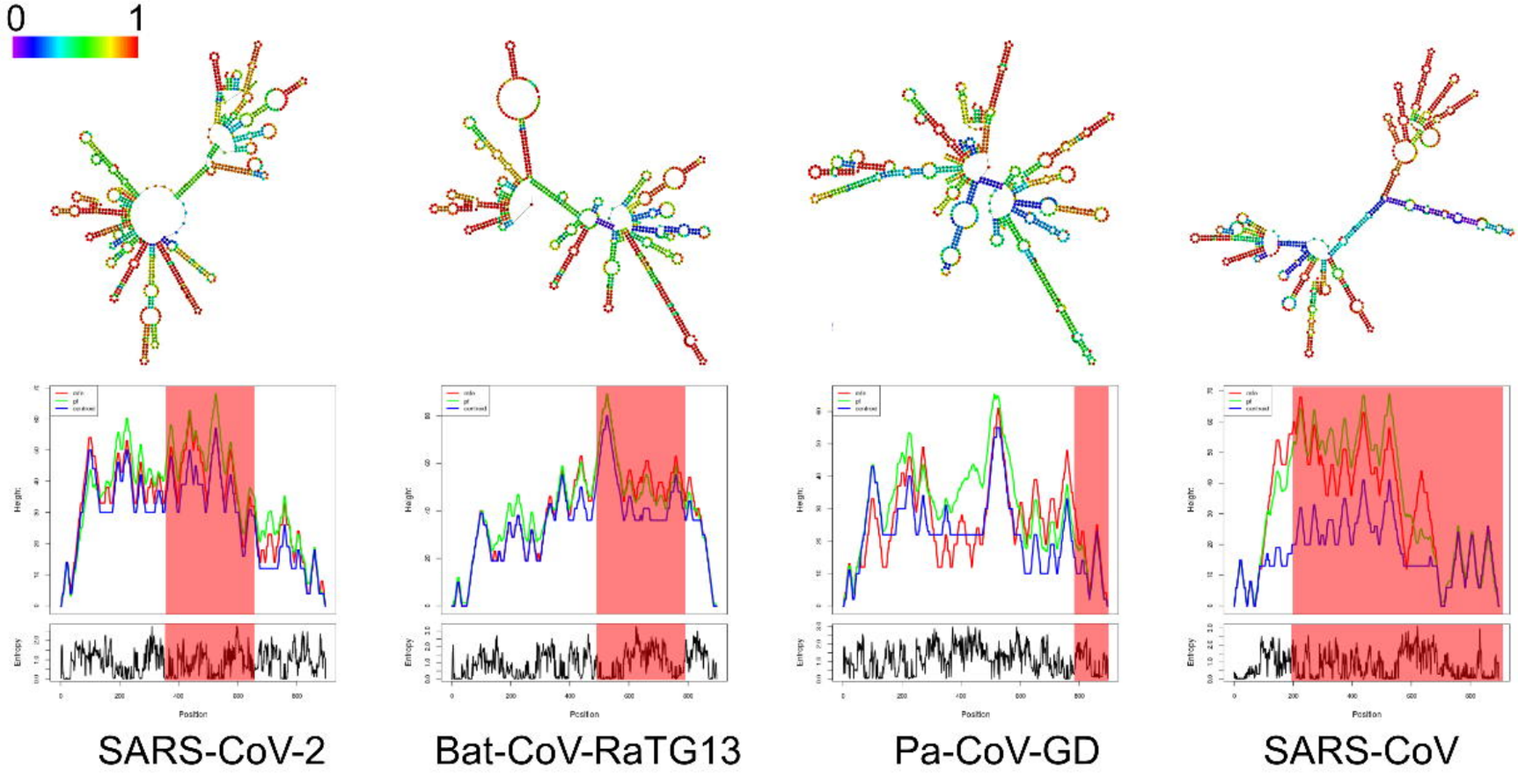
0
1
SARS-CoV-2
Bat-CoV-RaTG13
Pa-CoV-GD
SARS-CoV

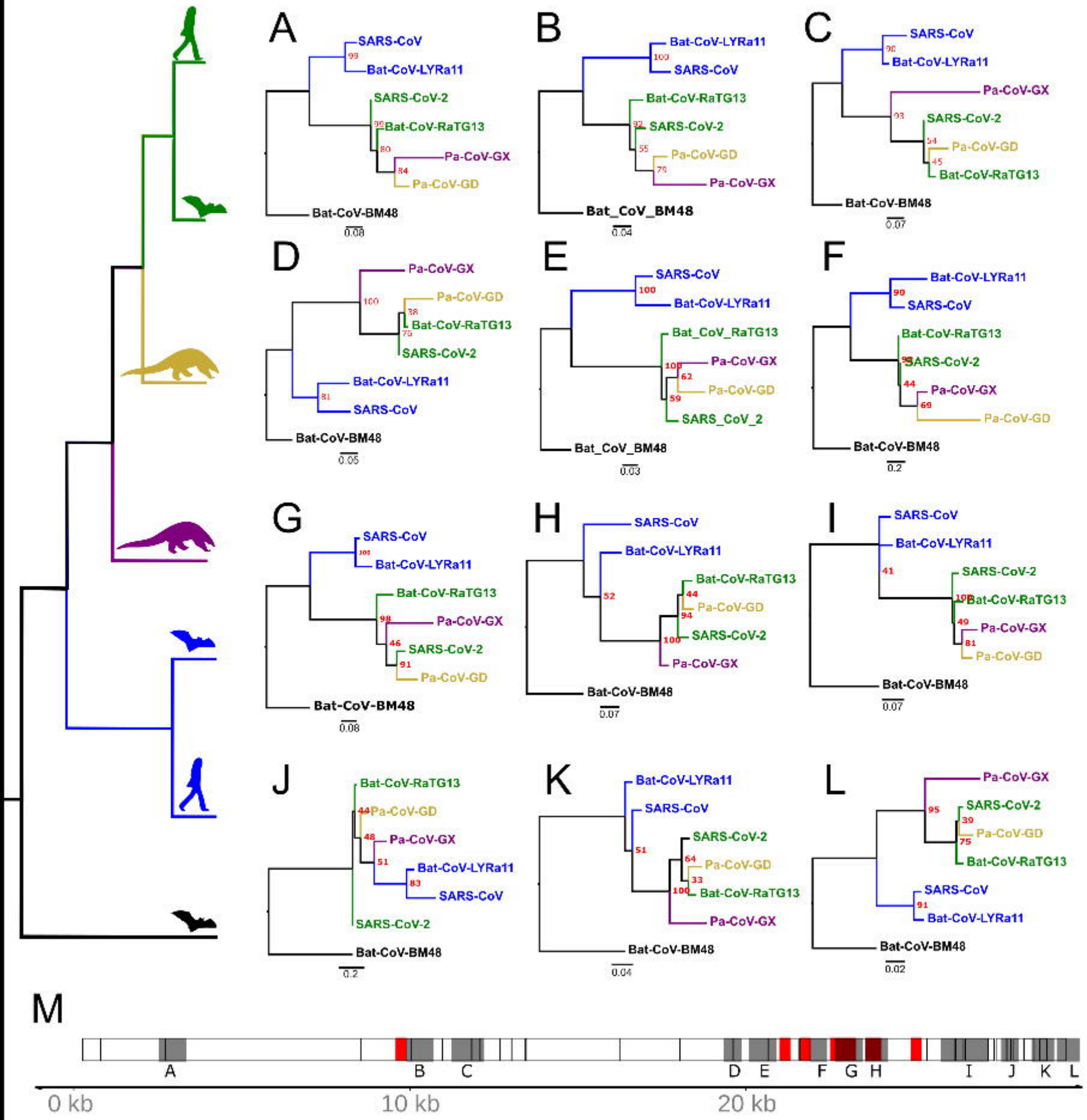
A
SARS-CoV
Bat-CoV-LYRa11
SARS-CoV-2
Bat-CoV-RaTG13
Pa-CoV-GX
Pa-CoV-GD
Bat-CoV-BM48
0.08
B
Bat-CoV-LYRa11
SARS-CoV
Bat-CoV-RaTG13
SARS-CoV-2
Pa-CoV-GD
Pa-CoV-GX
Bat_CoV_BM48
0.04
C
SARS-CoV
Bat-CoV-LYRa11
Pa-CoV-GX
SARS-CoV-2
Pa-CoV-GD
Bat-CoV-RaTG13
Bat-CoV-BM48
0.07
D
Pa-CoV-GX
Pa-CoV-GD
Bat-CoV-RaTG13
SARS-CoV-2
Bat-CoV-LYRa11
SARS-CoV
Bat-CoV-BM48
0.05
E
SARS-CoV
Bat-CoV-LYRa11
Bat_CoV_RaTG13
Pa-CoV-GX
Pa-CoV-GD
SARS_CoV_2
Bat_CoV_BM48
0.03
F
Bat-CoV-LYRa11
SARS-CoV
Bat-CoV-RaTG13
SARS-CoV-2
Pa-CoV-GX
Pa-CoV-GD
Bat-CoV-BM48
0.2
G
SARS-CoV
Bat-CoV-LYRa11
Bat-CoV-RaTG13
Pa-CoV-GX
SARS-CoV-2
Pa-CoV-GD
Bat-CoV-BM48
0.08
H
SARS-CoV
Bat-CoV-LYRa11
Bat-CoV-RaTG13
Pa-CoV-GD
SARS-CoV-2
Pa-CoV-GX
Bat-CoV-BM48
0.07
I
SARS-CoV
Bat-CoV-LYRa11
SARS-CoV-2
Bat-CoV-RaTG13
Pa-CoV-GX
Pa-CoV-GD
Bat-CoV-BM48
0.07
J
Bat-CoV-RaTG13
Pa-CoV-GD
Pa-CoV-GX
Bat-CoV-LYRa11
SARS-CoV
SARS-CoV-2
Bat-CoV-BM48
0.2
K
Bat-CoV-LYRa11
SARS-CoV
SARS-CoV-2
Pa-CoV-GD
Bat-CoV-RaTG13
Pa-CoV-GX
Bat-CoV-BM48
0.04
L
Pa-CoV-GX
SARS-CoV-2
Pa-CoV-GD
Bat-CoV-RaTG13
SARS-CoV
Bat-CoV-LYRa11
Bat-CoV-BM48
0.02
M
A
B
C
D
E
F
G
H
I
J
K
L
0 kb
10 kb
20 kb